Il Quaternario
7 (2), 1994, 577-588

FAULT INVERSION: AN EXAMPLE IN CENTRAL APENNINES (ITALY)

V. Bosi[1] - R. Funiciello[2] - P. Montone[1]
[1] Istituto Nazionale di Geofisica, Roma
[2] Dipartimento di Scienze Geologiche, III[a] Università di Roma, Roma

ABSTRACT - *Fault inversion: an example in central Apennines (Italy)* - Il Quaternario, 7(2), 1994, 577-588 - Phenomena related to large scale fault inversion have been observed on the basis of geological and structural evidence in the Central Apennines, along the northern extension of southwestern margin of Mt. Velino, 20 km east from L'Aquila (Central Italy).Two main tectonic events have been recognized by macro and mesostructural analyses. The compressional tectonic phase developed in Late Miocene-Early Pliocene produced thrusting of carbonate units onto Late Miocene-Messinian ones. Related to this tectonic event, high and low angle reverse faults have been identified, linked to a NW-SE and N-S trending thrust systems. During the following extensional phase, NW-SE trending faults began to be active and high angle NW-SE striking reverse faults were reactivated as normal faults with a very small left-lateral component. This last tectonic event probably developed during Early-Middle Pleistocene as was hypothesised in neighbouring areas. Between these two events, transpressional tectonics produced NW-SE left lateral faults which displaced the pre-formed thrust faults. Great portions of the ancient thrust planes are now exposed consequent to the final extensional movement that generated "fault slope features".

RIASSUNTO - *Riattivazione di* thrust *come faglie normali: un esempio nell' Appennino centrale (Italia)* - Il Quaternario, 7(2), 1994, 577-588 - Nell'Appennino centrale, lungo il prolungamento settentrionale del margine sud-orientale del Monte Velino, 20 km ad est di L'Aquila, sono stati identificati, mediante analisi geologiche e macro- e mesostrutturali, dei fenomeni di riattivazione di rampe di *thrust* come faglie normali. Sono stati riconosciuti due eventi tettonici principali: (a) un evento tettonico compressivo di età Miocene superiore-Pliocene inferiore che ha prodotto il sovrascorrimento di unità carbonatiche sopra le unità terrigene del Miocene superiore-Messiniano mediante faglie inverse a basso ed alto angolo legate a sistemi di *thrust* orientati NW-SE e N-S. Il secondo evento (b), a carattere distensivo ha prodotto la riattivazione delle rampe di *thrust* ad alto angolo come faglie normali a debole componente trascorrente sinistra. Questo secondo evento tettonico si è sviluppato, probabilmente, durante il Pleistocene inferiore-medio, come ipotizzanto anche in aree attigue. Faglie trascorrenti sinistre a direzione NW-SE che dislocano i suddetti sistemi di *thrust* sono state attribuite ad una fase transpressiva intermedia. Gli ultimi movimenti distensivi (b) hanno generato dei "versanti di faglia" che rappresentano ampie porzioni delle antiche rampe di *thrust*.

Key words: Structural geology, Pleistocene fault inversion, central Apennines, Italy
Parole chiave: Geologia strutturale, riattivazione di faglie, Pleistocene, Appennino centrale, Italia

1. INTRODUCTION AND GEOLOGICAL SETTING

The Central Apennines is a NW-SE to N-S trending post-collisional fold and thrust belt, built up mainly during Late Miocene-Early Pliocene. It is formed by different meso-Cenozoic palæogeographic units (Parotto, 1979; Parotto & Praturlon, 1975). These domains (namely, the Umbro-Marchean basin, a transitional domain (Sabina) and the Latium-Abruzzo carbonate platform) have been overthrusted onto each other and onto synorogenic terrigenous deposits, with an east-northeastern orogenic transport direction. Starting from late Tortonian times the migration of the rift basin–thrust belt–foredeep system toward the present Po–Adriatic–Ionian foreland caused the extension and compression of the Tyrrhenian and Adriatic sea margins, respectively (Patacca & Scandone, 1990).

The extensional tectonic phase took place in a geological environment characterized by thin skinned tectonics dominated by mainly NW-SE and N-S striking thrusts.

In this environment, the possible reactivation of thrust faults as normal faults, which could have played an important role on the subsequent evolution of the Latium-Abruzzo region, has to be considered very carefully. In different geological domains tectonic structures may be in fact strongly influenced by pre-existing inherited structures. Examples of intracontinental deformations accommodated by the reactivation of pre-existing faults rather than by the nucleation of new more favourably oriented fault systems are well known (Sykes, 1978, Brewer & Smithe, 1984; White *et al.*, 1986; Gillchrist *et al.*, 1987; Dixon *et al.*, 1987, Krantz, 1991). Reactivation phenomena have been studied in relation to mechanical parameters — pore-pressure, orientation and amount of dip of pre-existing structures for frictional reactivation with respect to stress tensor orientation, finite cohesive strength, critical stress difference (Sibson, 1985; 1990; Ivins *et al.*, 1990; Ranalli & Yin, 1990; Buchanan & McClay, 1991; Mitra & Islam, 1994), influence of depth (Huyghe & Mugnier, 1992) — which are significant for stability analyses applying the Coulomb-Navier fracture criterion.

Near the investigated area, examples of fault reactivation have already been hypothesized by Nijman (1971) for the south-western slope of Velino mountain and for the Magnola mountains (a kind of tectonic and gravity "collapse"), and by Mariotti & Capotorti (1988) in the "Fiamignano Fault" (back-sliding due to gravity), which is located on the north-western continuation of the structure here described.

The aim of this paper is to present an example of fault inversion phenomena in the central Apennines, which depends

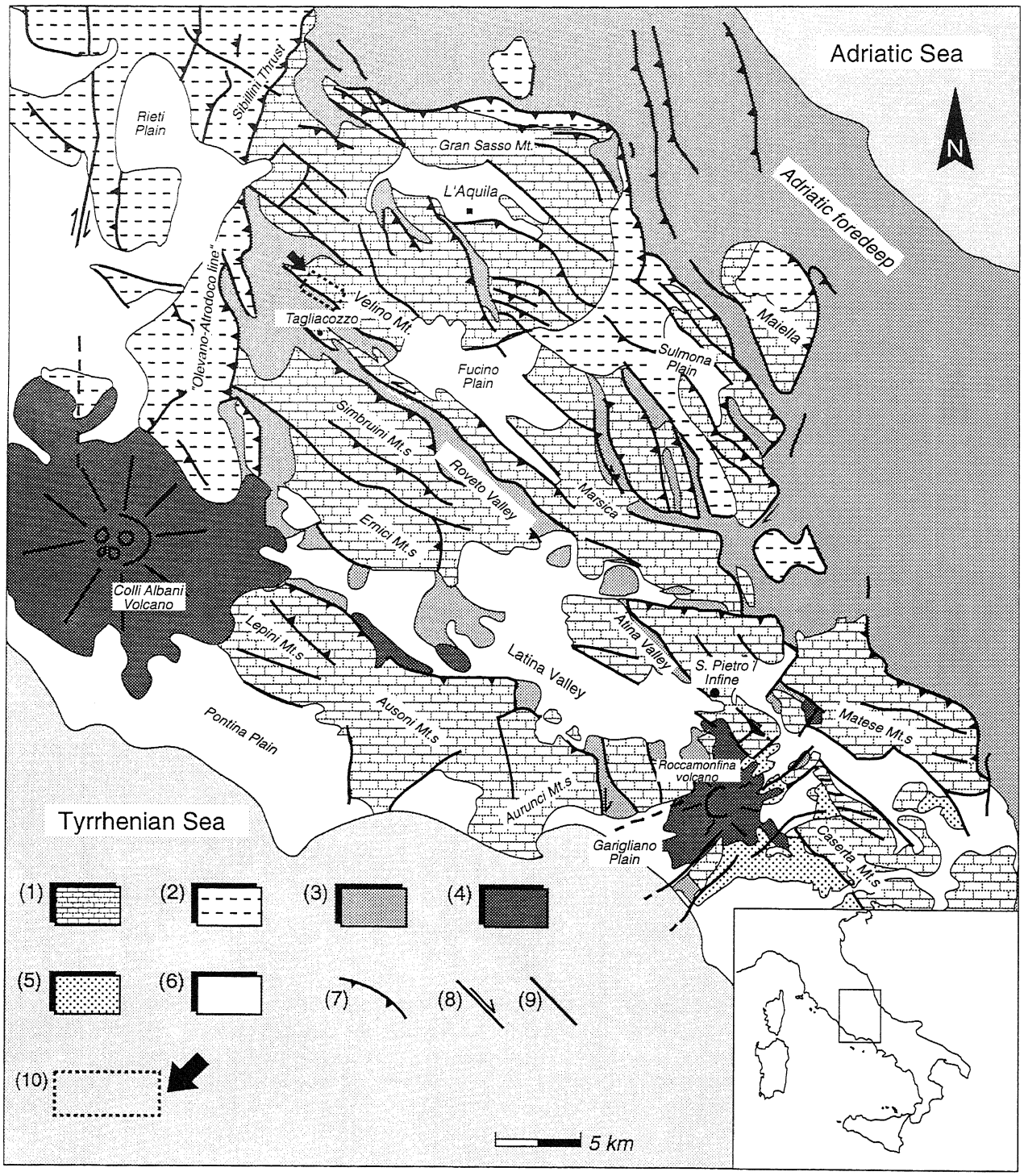

Fig. 1 - Schematic geological map of the Lazio-Abruzzi region and neighbouring areas. 1) Carbonatic units of the Lazio-Abruzzi platform (upper Trias-Lower Miocene); 2) Umbro-Sabina and Maiella transitional units (upper Trias-Upper Miocene); 3) Terrigenous deposits of the Latium-Abruzzo units (Tortonian-Messinian), the Adriatic Foredeep (Messinian-Pleistocene) and of the Molisan Basin (Upper Cretaceous-Messinian); 4) Volcanic deposits of Vesuvius (Upper Pleistocene-Holocene), Roccamonfina (Middle-Upper Pleistocene) and Alban Hills (Middle-Upper Pleistocene) volcanoes; 5) Pyroclastic deposits of the Phlegræan Fields eruption (Upper Pleistocene); 6) Continental and marine deposits of coastal and intramontane basins; 7) Thrust faults; 8) Strike-slip faults; 9) Normal faults; 10) Location of the studied area.

Carta geologica schematica della regione laziale-abruzzese ed aree attigue. 1) Unità carbonatiche di piattaforma laziale abruzzese (Trias sup.-Miocene inf.); 2) Unità di transizione Umbro-sabina e della Maiella (Trias sup.-Miocene sup.); 3) Depositi terrigeni laziali-abruzzesi (Tortoniano-Messiniano), di Avanfossa (Messiniano-Pleistocene) e del Bacino molisabo (Cretacico sup.-Messiniano); 4) De-positi vulcanici del Vesuvio (Pleistocene sup.-Olocene), del Roccamonfina (Pleistocene medio-superiore), e dei Colli Albani (Pleistocene medio-superiore); 5) Depositi piroclastici dei Campi Flegrei (Pleistocene superiore); 6) Depositi marini e continentali di depressioni costiere e intramontane; 7) Sovrascorrimenti; 8) Faglie trascorrenti; 9) Faglie normali; 10) Area studiata.

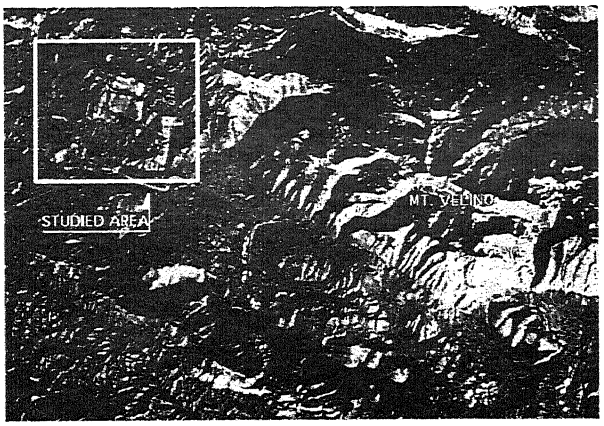

Fig. 2 - False colour composite photo of a Lansat image of the studied area (squared). Composition of bands 4-5-7; a non-directional edge enhancement was also applied. Processing by S. Salvi (I.N.G.). Mt. Velino is the prominence in the centre right of the photo.

Immagine Landsat dell'area studiata (nel riquadro). Composizione delle bande 4-5-7. Elaborazione di S. Salvi (I.N.G.). Il Monte Velino è visibile nella parte centrale destra della foto.

substantially on the original dip-angle of pre-existing thrust planes and on friction angle.

We performed (a) a detailed field survey (scale 1:10,000) based on a litho-stratigraphic analysis (100 thin sections have been observed by optical microsope) and on the identification of morphological features by aerial photos at different scales (1:70,000÷1:33,000), (b) a structural analysis of the tectonic elements as recognized at macro- and mesoscale, and (c) micro-structural observations (SEM) on portions of the main fault planes in order to recognize the sense of motion. These analyses have given results which are in favour of fault inversion phenomena.

The investigated area is located 80 km east of Rome and 10 km north-west of Fucino Plain, to the east of the "Olevano-Antrodoco" fault zone (Fig. 1) where the Sabina units are thrusted onto the Latium-Abruzzi units. Morphologically the area can be divided into three sectors (Fig. 2): (A) and (C) on the right and left end, which range 775÷820 m (A) and 960÷1200 m (C) in elevation and are characterized by two wide areas (Borgorose depression and Malito valley) filled by terrigenous deposits (Upper Tortonian-Messinian); and (B), with a rough morphology ranging 900÷1650 m in elevation. The latter is characterized by narrow closed valleys which separate the NW-SE trending carbonate main mountain ridges (Mt. Castiglione-Mt. Costa; Mt. Calata-Mt. Macello; Mt. Maglia Cupa-Mt. Fratta), which are formed of different tectonic units overthrusted on one another. These tectonic units are made up of a stratigraphic succession belonging to the Latium-Abruzzi carbonatic sequence (Parotto & Praturlon, 1975; Accordi *et al.*, 1988), including stratigraphic successions ranging in age from Early Cretaceous to Late Miocene (in outcrop).

The regional structural setting is characterized by NW-SE trending rigid tectonic blocks separated by prevailingly sub-parallel fault systems, which played an important role after thrusting (Salvini, 1992), and on which left-lateral strike-slip and dip-slip movements have been recognized (Montone & Salvini, 1991). Interaction among these fault systems caused a series of deformational structures (recognizable along fault-block margins) even in Quaternary times (Galadini & Messina, 1993).

2. ANALYSIS OF DATA COLLECTED

2.1 Stratigraphic elements

The local stratigraphic succession is made up of calcareous-dolomitic and oolitic-algal limestones (Early Cretaceous) ranging in age from Aptian (*Pianella dinarica*, requienids, and some caprinids) to Middle Cenomanian (*Sellialveolina vialli*). On the top of the succession, small lenses of bauxite with benthonic Foraminifera and Ostracoda (Cretaceous-Palæocene) indicate the uplifting of the carbonate platform.

After the palæogenic *hiatus,* the succession continues in apparently angular conformity with a detrital organic limestone (*"Calcari a Briozoi e Litotamni"*) of Early Miocene. Grey marls and marly limestones (*"Marne ad Orbuline"*) (Serravallian-Tortonian in age) testify the beginning of the Apennines' orogeny. The stratigraphic boundary between the two formations is characterized by a typical thin level of conglomerate, rich in glauconite.

The end of the meso-Cenozoic succession is marked by clayey-arenaceous flysch deposits (Late Tortonian-Messinian), covered by continental sequences with ancient terraced alluvial deposits, alluvial fan deposits and slope breccias.

In the southwestern end of the area, a clastic unit including a thick well-stratified succession of gravel and conglomerates, displaying parallel and cross laminations has been recognized; bedding and imbrication of pebbles suggest an E-SE provenance. Toward the west, the size of pebbles in the stratigraphic sequence gradually decreases as well as interposition of sand and silt levels, which strenghtens the hypothesis of the E-SE provenance of deposits. This sedimentary unit probably represents the progressive infilling of an intramontane basin, located on the right of River Salto, and may probably be correlated with the "Upper Villafranchian" conglomeratic succession observed in the nearby Rieti basin (Cavinato, 1989; 1993).

2.2 Macro-structural features

Boundaries between carbonate tectonic units are fault systems, often displaying a complex tectonic evolution.

On the eastern side of the area, NW-SE and N-S striking thrusts dipping 15÷20° westward have been recognized on the basis of stratigraphic offsets and of kinematic indicators on fault planes (calcite slickenside and

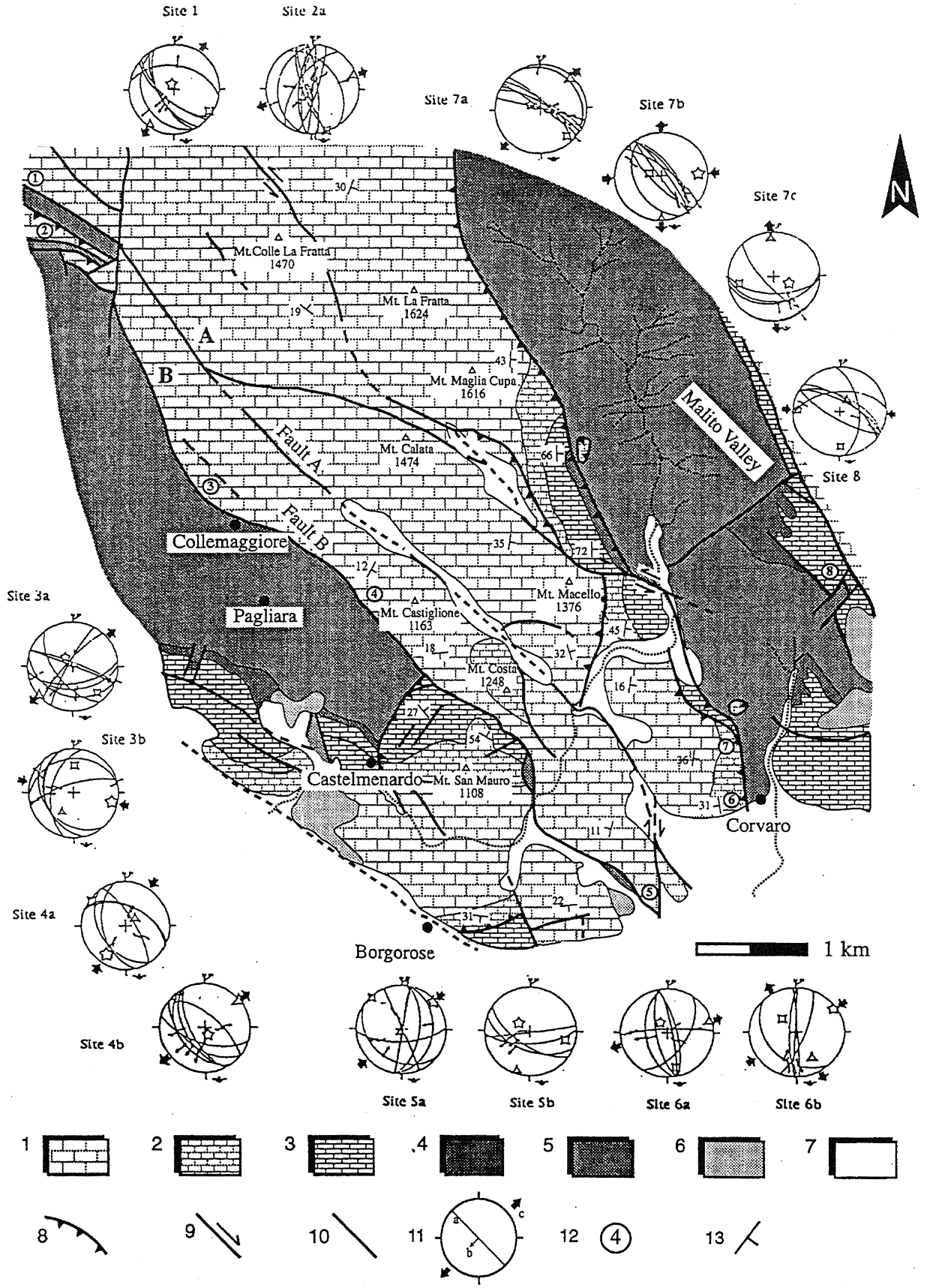

Fig. 3 - Geological and structural map of the study area. Faults A and B represent thrust planes reactived as normal faults. 1) Stratified limestone and dolomitic limestone, ooid or skeletal packstone (Lower Cretaceous); 2) Stratified limestone and dolomitic limestone with benthonic Foraminifera and rudist debris (Upper Cretaceous-Paleocene); 3) Detrital organic limestone with pelagic and *(cont.)* →

steps, stylolitic peaks, frictional-wear grooves), if the following criteria for identifying sense of slip on fault planes well described in Angelier (1984). These NW-SE and N-S trending structures, which separate the Mt. Maglia Cupa-Mt. Macello ridges from the Malito Valley, are relatively continuous along strike (Fig. 3). The best exposed thrust plane outcrops just to the north of Corvaro (N 139° 28°SW, pitch 67°). To the west, the Mt. Macello, Mt. Costa and Castelmenardo tectonic units are overlapped with low angle SW dipping (35÷40°) normal faults. These faults cut all previous structures and outcrop for 3÷5 km and coincide with the south-western slopes of the Mt. Costa and Mt. Macello ridges, giving a planar shape to the slopes (Fig. 4). Along the fault planes two different motion senses have been recognized. Reverse movements are well defined by either thinly deformed terrigenous levels, or widely deformed levels (Tortonian-Messinian) which are tectonically interposed between Mt. San Mauro, Mt. Castiglione and Mt. Macello ridges (made up of Lower Cretaceous-Lower Miocene carbonatic successions), and by a complex compressive geometry formed by N-NE verging folds and NW-SE striking minor thrusts, visible near Castelmenardo. Late normal displacements along these same faults (N 137° 39°SW, pitch 82°) have been identified on the basis of actual stratigraphic offsets (more than 500 m on the "Mt. Castiglione-Mt. Costa fault plane"; Figs. 3 and 4) and of the slip sense on fault planes (Fig. 6). In particular, a general decrease of the normal stratigraphic offset toward SE is recognizable. The final normal displacement increases in fact to the north (see Fig. 3).

These macrostructural features indicate that only thrust planes dipping more than 35° would be reactivated as normal faults. Such a dip-angle value is in agreement with the minimum expected dip angle of experimental models (Faccenna *et al.*, 1994). The structural pattern is complicated by NW-SE trending left-lateral faults with a minor vertical component (Fig. 3), connected with the compressional phase and in some cases reactivated as normal dip-slip faults. These strike-slip faults displaced the main thrust fronts by which the Mt. Maglia Cupa carbonate unit overthrusted onto the flysch sequence (Malito Valley).

On the south-western end of the area, where the Mt. San Mauro carbonatic unit (meso-Cenozoic in age) seems to be overthrusted onto the "Pagliara Flysch " unit (Upper Tortonian-Messinian), the carbonate sequence overlies the terrigenous deposits outcropping to the north-east of Castelmenardo. These units are cut by NE-SW striking discontinuities among which we did not observe clear thrust planes and high deformational zones. It is worth noting that main faults on the NW slope of Mt. San Mauro are NE-SW trending and show normal displacements. An interpretation of these macrostructural features will be given in the conclusions.

2.3 Meso-structural analysis

During structural analysis, features of brittle deformation such as fractures and fault planes which affected the meso-Cenozoic stratigraphic succession at the meso-scale have primarily been taken into account; the Quaternary deposits do not seem to be affected by faulting.

Measurement sites have been located along or near major structures. Site locations and main results are shown in Figure 3. More than 1100 measurament data have been introduced into the analysis using Angelier's method (Angelier, 1984; 1990). This method allows the reconstruction of palæostress axes σ1, σ2 and σ3 (maximum, intermediate and minimum stress, respectively) and of the ratio $F = \sigma2-\sigma3/\sigma1-\sigma3$, between magnitude of principal stress, known orientation and sense of slip on faults acting during the same tectonic event. Principles, limits and application conditions of this method are described in Angelier (1984; 1990). Figure 6 shows examples of identification of the sense of slip on a fault plane; our analysis is based on such data.

The statistical analysis of data collected, most of which refers to strike, dip and pitch of fault planes and to strike and dip of joints, shows two main tectonic events:

(a) a compressional tectonic phase with NE-SW maximum compressional orientation (σ1), which caused NW-

---

benthonic fauna [Briozoans, Echinoids, Lithotamnia, Corals (Middle Miocene)]; 4) Gray marl and marly limestone, thinly bedded with planktonic Foraminifera (Serravallian-Tortonian); 5) Thick bedded sandstone; locally silty arenaceous turbiditic successions (Upper Tortonian-Messinian); 6) Continental deposits: lacustrine deposits, slope breccias, clayey-ochraceous *"terra rossa"*, doline floor deposits, palæosols (Plio-Pleistocene); 7) Recent alluvial deposits: sand, gravel and conglomerates; 8) Thrust fault; 9) Strike-slip fault; 10) Dip-slip fault; 11) Schmidt diagram (lower hemisphere): a) fault plane, b) striae, c) stress tensor axes: σ1 and σ3 directions ; 12) Site of meso-structural analyses; 13) Bedding.

Carta geologico-strutturale dell'area studioata. Le faglie A e B rappresentano i piani di sovrascorrimento che sono stati riattivati come faglie normali. 1) Calcari e calcari dolomitici stratificati, oolitici e organogeni (Cretacico inf.); 2) Calcari stratificati e calcari dolomitici con Foraminiferi bentonici e rudiste (Cretacico sup.-Paleocene); 3) Calcari detritico-organognei con fauna bentonica e pelagica [Briozoi, Echinidi, Litotamni, Coralli (Miocene medio)]; 4) Marne e marne calcaree grigiastre con sottili livelli di Foraminiferi planctonici (Serravalliano-Tortoniano); 5) Arenarie in banchi e successioni torbiditiche arenaceo-limose (Tortoniano sup.-Messiniano); 6) Depositi continentali: depositi lacustri, brecce di pendio, "terre rosse", depositi di dolina e paleosuoli (Plio-Pleistocene); 7) Depositi alluvionali recenti: sabbie, ghiaie e conglomerati; 8) Sovrascorrimenti; 9) Faglie trascorrenti; 10) Faglie normali; 11) Diagramma di Schmidt (ermisfero inferiore): a) piano di faglia, b) strie, c) assi del tensore degli sforzi: direzione di σ1 e σ3; 12) Stazioni di analisi mesostrutturale; 13) Immersione degli strati.

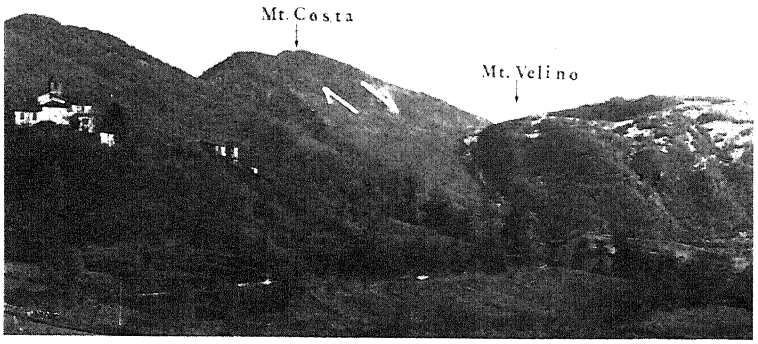

Fig. 4 - Southwestern slope of Mt. Castiglione - Mt. Costa mountain ridge. The slope coincides with a NW-SE striking low angle normal fault. View from the town of Collemaggiore. Arrows point out the Mt. San Mauro double (reverse and normal) sense of motion.

Versante sud-orientale della dorsale di M. Castiglione-M. Costa. Il versante coincide con una faglia normale a basso angolo a direzione NW-SE. Vista dall'abitato di Collemaggiore. Le frecce mettono in luce il doppio senso di movimento di M. San Mauro (inverso e normale).

SE and N-S striking thrust faults (dip 10°/15°÷ 35°/40°) and probably NW-SE striking left-lateral faults (Fig. 3, sites 3b, 4a, 5a, 6b, 7b, 8). Kinematic indicators are mainly represented by stylolitic and mechanical striations. The locally observed orientation of the maximum stress tensor axis, ranging from N220° to N280° (Fig. 3), may be the effect of either σ1 rotation or block-rotation phenomena. With the latter, the stress tensor direction may probably be considered as an apparent direction even if no palæomagnetic data about block-rotations around a vertical axis are available in the area. However, interference phenomena and local refraction of stress tensor axes have been taken into account and will be discussed below. A temporal relationship between the NW-SE thrust and strike-slip faults has been observed only on the eastern side of the area where a N 125° striking left-lateral strike-slip fault cuts an older N-S striking thrust, as testified by field observations (kinematic indicators and horizontal displacement of the stratigraphic units);

(b) a subsequent extensional tectonic phase (Fig. 3) caused NW-SE trending neoformed normal faults (dip 60°÷70°) which cut previous structures, and NW-SE striking low angle normal faults dipping 35°÷40°. The results (sites 1, 2a, 3a, 4b, 5b, 6a, 7a) show a rather homogeneous NE-SW direction of minimum compression (σ3) in the whole area. Kinematic indicators are represented by calcite slickensides and mechanical striations.

The time relationship between NW-SE striking reverse and normal faults has clearly been observed, especially in the southern part of the studied area.

2.4 Micro-structural analysis

Oriented samples have been collected for analysis along fault planes to identify the relative sense of motion which occurred in the past.

Analysis was carried out using both optical and scanning electron (SEM) microscope, which allow a semi-quantitative analysis of the rock and slikenside chemical components and the collection of data on slip-vectors from 40 out of 45 observed samples. Three kinds of kinematic indicators have been observed (Patterson, 1958; Hancock, 1985; Angelier, 1991; Montone, 1990): a) calcite striations due to growth of calcite fibres on the

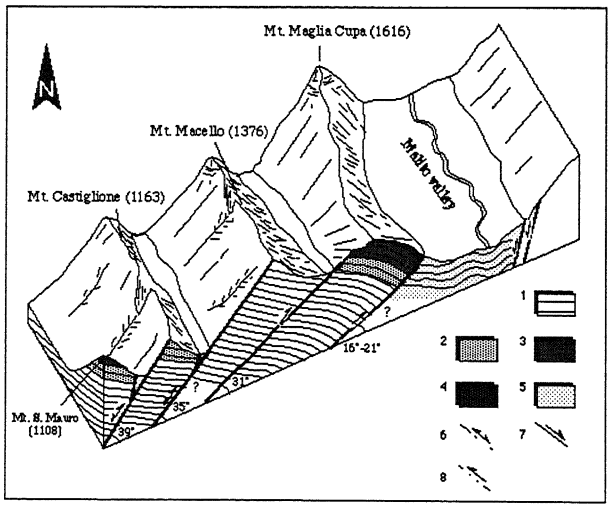

Fig. 5 - Schematic block-diagram of the central part of the study area (not in scale) 1) Early Cretaceous limestone; 2) Upper Cretaceous limestone; 3) Middle Miocene limestone; 4) Serravallian-Tortonian grey marl; 5) Upper Tortonian-Messinian terrigenous deposits; 6) Faults with double sense of slip; 7) Normal fault; 8) Thrust fault. The minimum dip-angle for the reactivation is about 35° (less than the expected dip-angle in the experimental models, which is greater than 39°÷40°). It is hypothesised that this depends on the presence of thin flysch levels among carbonatic units favouring a friction angle decrease along fault zones.

Block-*Diagramma del settore centrale dell'area studiata (non in scala). 1) Calcari del Cretacico inf.; 2) Calcari del Cretacico sup.; 3) Calcari del Miocene medio; 4) Marne grigiastre del Serravalliano-Tortoniano; 5) Depositi terrigeni del Tortoniano superiore-Messiniano; 6) Faglie con doppio senso di movimento; 7) Faglie normali; 8) Sovrascorrimenti. L'angolo minimo di riattivazione è circa di 35° (minore dell'angolo riscontrato in modelli sperimentali valutato in circa 39°÷40°. Questa circostanza è secondo noi dovuta alla presenza di sottili livelli di flisch interposti tra le dorsali carbonatiche che diminuiscono il coefficiente di frizione lungo le zone di faglia.*

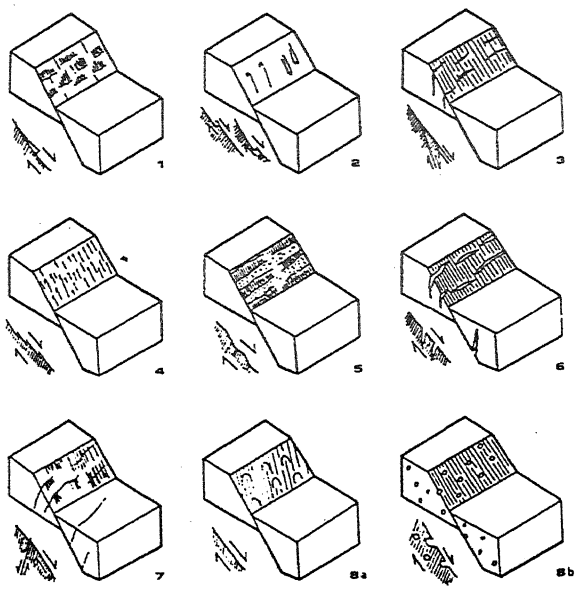

Fig. 6 - Criteria for determining the sense of motion on a fault plane. 1) Calcite steps; 2) Tectonic toolmarks; 3) Riedle shears; 4) Stylolitic peaks; 5) Alternating polished and rough facets; 6) Tension gashes; 7) Conjugate shear fractures; 8) Miscellaneous criteria: (a) parabolic marks and (b) deformed bubbles in lava. From Angelier (1991).

Criteri per la determinazione del senso di movimento su un piano di faglia. 1) Scalini di calcite; 2) Marchi tettonici; 3) Fratture di Riedle; 4) Picchi stilolitici; 5) Fasce ruvide e lisce alternate; 6) "Tension gashes"; *7) Fratture di taglio coniugate; 8) (a) strutture paraboliche e (b) deformazioni in lava. Da Angelier (1991).*

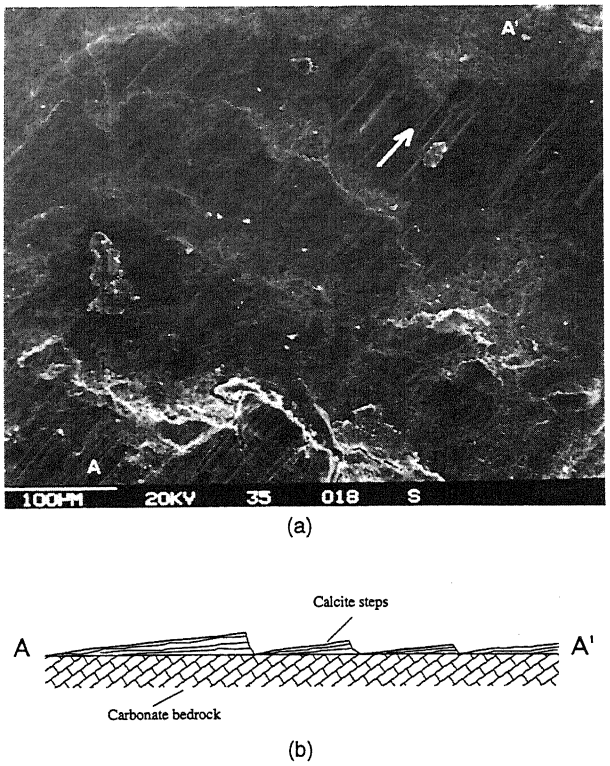

Fig. 7 - (a) SEM view of calcite striae and steps on a fault plane. A-A': Motion sense is shown by the arrow; (b) A-A': section of calcite steps and fibres.

(a) Immagine SEM di strie e scalini di calcite sul piano di faglia. A-A': La freccia indica il senso del movimento; (b) A-A': sezione di fibre e scalini di calcite.

fault plane (Fig.7); b) stylolitic peaks induced by pressure-solution phenomena; and c) mechanical striations (grooves) induced by abrasion be-tween hangingwall and footwall of the fault (Fig. 8).

The analysis, performed on 23 samples of low angle normal faults, shows two slickenside orientations with same direction and opposite sense of motion that may be due to fault inversion phenomena. In this case, slickensides relative to normal movements, are overlapped to the others testifying the reactivation of high-angle reverse faults as normal faults. Moreover, up to 4 different slickenside orientations probably induced by the rotation of little blocks inside the main fault zones, have been recognized on secondary fault planes.

When kinematic indicators are not perfectly clear (especially in mechanical grooves) these have not been considered and analyses to test the validity of microstructural observations have been performed only when stratigraphic displacements are well defined.

Microstructural analysis has been applied on the fault planes observed during mesostructural studies: this technique allows the collection of data on the sense of motion from 40 out of 45 samples, on which mesoscale kinematic indicators are not visible. Thus, this method has resulted to be useful to gather data which cannot be observed in the field.

3. DISCUSSION AND CONCLUSIONS

The results from both field and laboratory analyses indicate that thrust faults as generated during a first compressional tectonic phase, would have been reactivated as low angle normal faults when an extensional tectonic event occurred. Evidence of fault reactivation is shown along faults A and B (Figs. 3 and 5); the late normal displacement is shown by stratigraphic offsets, while reverse movements are well de-fined by the thin terrigenous levels which are interposed among the Mt. San Mauro - Mt. Castiglione - Mt. Macello mountain ridges along the faults that separate these three ridges. In particular, only high-angle thrust planes dipping 39÷35° were reactivated on the western side of the area. Low-angle thrust planes were not involved in reactivation and were cut by NW-SE trending neoformed normal faults (dipping 55÷65° westward) and N125° striking subvertical left-lateral faults. These results are in relatively good agreement with theoretical and analogic models which tend to show no reactivation on fault planes dipping less than 35° (Faccenna *et al.*, 1994).

Late normal displacements along the same faults have been recognized on the basis of identified strat-

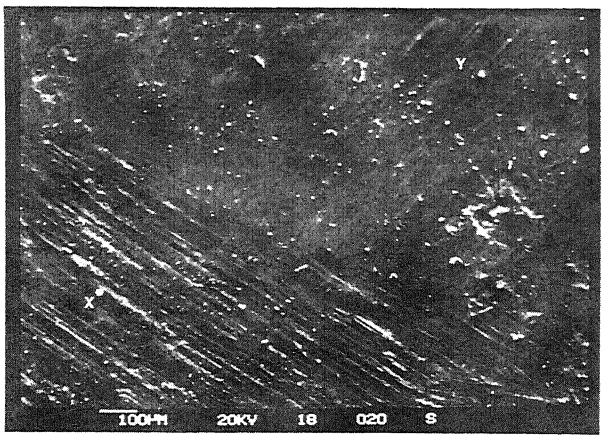

Fig. 8 - SEM view of mechanical abrasion striations, on a secondary fault close to fault A. The temporal relationship between the two orientations are clearly showed (X younger than Y).

Immagine SEM di strie di abrasione meccanica su un piano di faglia secondario, attiguo alla faglia A. La relazione di antecedenza tra le due orientazioni è chiara (X più giovane di Y)

igraphic offsets (more than 500 m along Mt. Castiglione/Mt. Costa fault) and by kinematic indicators. Figure 9 (a, b) show a schematic fault tectonic inversion along the two western structures.

On the basis of this data the apparent NE-SW striking thrust fault observed near Castelmenardo was caused probably by reactivation and consequent back-sliding of the Mt. San Mauro block along the Mt. Costa-Mt. Castiglione normal fault.

The age of reactivation taking into account only our data is not well constrained, mainly because of the lack of post-Messinian-Late Pliocene sediments. In addition, Early-Middle Pleistocene deposits outcrop discontinuously and not close to the fault zones. Nevertheless, on the basis of an analogy in the shape and amount of normal displacement between studied faults (Fig. 10) with the nearby Velino fault, which represents a normal reactivation of an ancient thrust plane starting from Early Pleistocene (Bosi & Federici, 1994), the last extensional tectonic event in the investigated area may reasonably be ascribed to the same period. A different freshness of morphology between fault A and B (the planar shape of A fault slope is less conserved) may indicate a more recent activity of fault B, even if no morphological evidence of recent movements dating from Upper Pleistocene to Holocene have been recognized along it.

With reference to the stress tensor orientation derived from mesostructural analyses, a post Tortonian-Messinian tectonic evolution is proposed, which would have developed by permutation of the three stress tensor axes as shown in Figure 11;the apparent rotation of the maximum compressive axis (σ1) in the second tectonic event (A') is due to the local stress tensor orientation, probably induced by N-S right-lateral shear zones, which caused block rotation phe-nomena along NW-SE striking faults with a left-lateral sense of motion. This counter-clockwise and clockwise rotation of rigid blocks can largely be observed in the Latium-Abruzzi region (Mattei *et al.*, 1991)

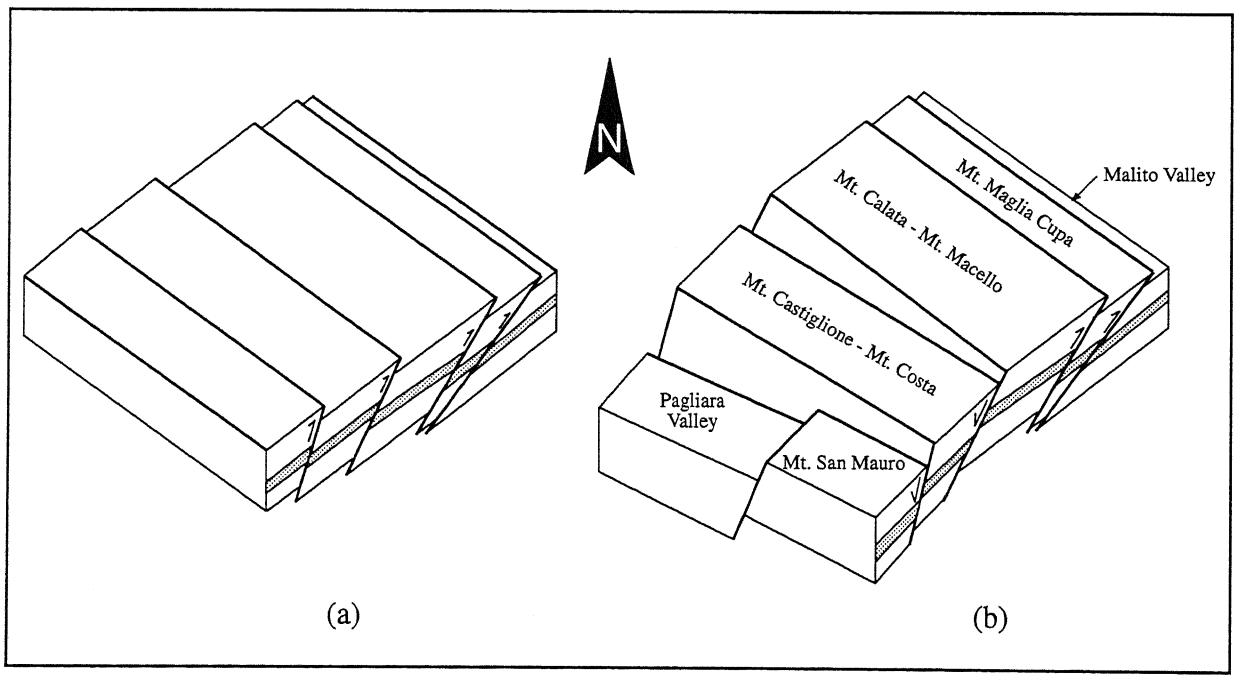

Fig. 9 - Schematic block diagram of fault inversion phenomena: a) after a compressional phase (A in Fig. 11); and b) after inversion phenomena. With the decrease of normal displacement toward southeast, kinematic indicators on the NW-SE normal faults show a very small left-lateral component because of the different amount of backsliding along these faults.

Block-*diagramma del fenomeno di inversione tettonica. a) dopo l'evento compressivo (A in Fig. 11); b) dopo il fenomeno di inversione. In conformità alla diminuzione del rigetto normale verso SE, gli indicatori cinematici sulle faglie normali a direzione NW-SE mostrano una piccola componente laterale sinistra, dovuta ad una diversa entità di retroscorrimento lungo tali faglie.*

Fig. 10 - "Fault slope" feature of the Mt. Velino ridge. Shape and dip angle of the fault plane are the same of the Mt. Castiglione - Mt. Costa southwestern slope (Fig 4).

Versante di faglia della catena del Velino. Forma e angolo di immersione del piano di faglia sono analoghi a quelli osservati lungo la dorsale Monte Costa-Monte Castiglione (Fig. 4).

depending on the location of the site with respect to the main shear zones. Even though no palæomagnetic data are available, nevertheless the counter clockwise rotation of the western tectonic units, as induced by different amounts of final normal displacement along the NW-SE striking fault planes, determination of the real value of the rotation angle is possible.

The problem of distinguishing between kinematic effects of gravitational "collapse" and extensional faulting, and of distinguishing which mesoscale and microscale structures would be diagnostic of backsliding due to gravity and which would be diagnostic of tectonic movements, is still a matter of discussion. However, there are indications that reactivation phenomena occurred in the investigated area, mainly due to tectonic instead of gravitational mechanisms :

– mesostructural analyses highlight the good agreement between slip directions of low-angle and high-angle normal faults, showing the presence of a stress field (B in Fig. 11) characterized by a NE-SW direction of extension (σ3) during thrust reactivation;

– the orientation of the σ3 axis is fairly constant (Fig. 3), even in areas not close to the studied sites (Fig. 3, sites 6 and 7);

– thrust planes dipping less than 35° are cut by NW-SE trending and 57÷65° dipping normal faults.

The presence of inversion phenomena in nearby areas such as the continuation of the studied structures, seems to support the above discussed hypothesis. In an extensional tectonics environment, because of the parallelism between σ1 and the gravity force, the results obtained are anyway insufficient to discriminate the influence of gravity from tectonic forces on the structures.

With regard to the unusually planar shape of "fault slopes" it is thought that, in spite of erosional phases which played an important role during Quaternary time, the original shape of these "fault-slopes" could keep intact

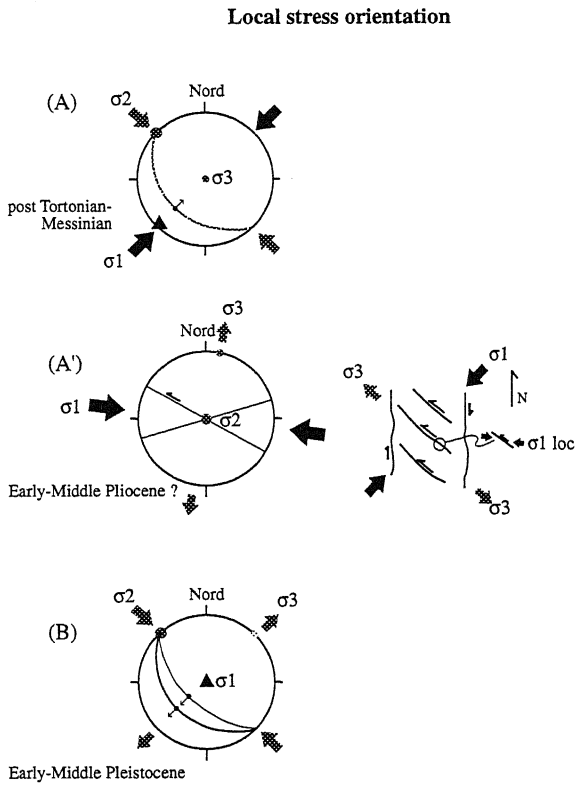

Fig. 11 - Tectonic evolution of the area as developed by permutation of the three stress tensor axes. The progressive increasing of the vertical component of tensor axes is probably due to the increasing in elevation of the mountain chain during thrusting together with the NE-SW extension of the Tyrrhenian margin. The anomalous orientation of stress tensor axes (A') is supposed to be due to local reorientations; regional stress tensor axes are shown on the right of (A')

Evoluzione tettonica dell'area sviluppatasi per la permutazione dei tre assi di sforzo. Il progressivo aumento della componente verticale del tensore è probabilmente dovuto all'incremento di quota della dorsale durante il thrusting *in concomitanza dell'estensione antiappenninica del margine tirrenico. L'anomala orientazione del tensore di sforzo A' è probabilmente collegabile a fenomeni di riorientazione locale; gli assi del tensore di sforzo regionale sono indicati sulla destra di A'.*

because (a) the original dip-angle is about the same with respect to the expected dip angle for carbonate slope retreat (Hirano, 1968), and (b) because reactivation reasonably happened in Lower Pleistocene.

Other two hypotheses should be taken into consideration:

– reactivation phenomena occurred in very recent times which could be still active, such as it was hypothesised for the Velino fault-slope (Bosi, 1975);

– the planar shape of the slope is due mainly to erosive processes that exhumed an old structure showing its original shape.

As far as the first hypothesis is concerned, no evidence of active faulting have been recognized in the area, apart from the apparent morphological freshness of faults. In terms of the second hypothesis, no progressive degradation of the planar shape from bottom to top of the fault plane has been observed, and — notwithstanding ramp-flat geometry is an usual feature in central Apennines — there is no evidence of such great exhumation phenomena in nearby areas.

REFERENCES

Accordi G., Carbone F., Civitelli G., Corda L., De Rita D., Esu D., Funiciello R., Kotsakis T., Mariotti G. & Sposato A., 1988 - *Note illustrative alla Carta delle litofacies del Lazio-Abruzzo ed aree limitrofe.* C.N.R. - P.F.G., Quad. Ric. Scient., 114, vol. 5.

Angelier J., 1991 - *Fault slip analysis and paleostress recontruction.* In: *Continental deformation* (Ed. by P.L. Hancock), Pergamon Press, 289-304.

Angelier J., 1990 - *Inversion of field data in fault tectonics to obtain the regional stress-III. A new rapid direct inversion method by analytical means.* Geophys. J. Int., **103**, 363-376.

Bosi C., 1975 - *Osservazioni preliminari su faglie probabilmente attive nell'Appennino centrale.* Boll. Soc. Geol. It., **94**, 827-859.

Bosi V. & Federici V., 1994 - *La conca di Corvaro.* In: *Guida all'Escursione alle Conche intermontane dell'Appennino Laziale-Abruzzese.* Il Quaternario, **6**(2), 393- 395.

Brewer J.A. & Smithe D.K., 1984 - *MOIST and the continuity of crustal reflectors along the Caledonian-Appalachian orogen.* J. Struct. Geology, **141**, 105-120.

Buchanan P.G. & McClay K.R., 1991 - *Sandbox experiment of inverted listric and planar fault systems.* Tectonophysics, **188**, 97-115.

D'Argenio B. 1966 - *Zone isotopiche e fagli etrascorrenti nell'Appennino centro-meridionale.* Mem. Soc. Geol. It., **5**, 279-299.

Dixon T.H., Stern R.J. & Hussein I.E., 1987 - *Controls of Red Sea rift geometry by Precambrian structures.* Tectonics, **6**, 551-571.

Faccenna C., Nalpas T., Brun J.P., Davy P. & Bosi V., 1994 - *The influence of pre-existing thrust planes on normal fault geometry: experimental modelling and geological examples.* J. Struct. Geol. (in press).

Galadini F. & Messina P., 1993 - *Stratigrafia dei depositi continentali, tettonica ed evoluzione geologica quaternaria dell'alta valle del fiume Sangro.* Boll. Soc. Geol. It., **112**.

Gillcrist R., Coward M. & Mugnier J.L., 1987 - *Structural inversion and its control.* Geodinamica Acta, **1**, 1-25.

Hancock P.L., 1985 - *Brittle microtectonics: principles and practics.* J. Struct. Geol., **7**, 3/4, 437-457.

Hirano M., 1968 - *A matematical model of slope development - an approach to the analytical theory of erosional topography.* J. Geosci. Osaka City Univ., **11**, 13-52.

Huyghe P. & Mugnier J.L., 1992 - *The influence of depth on reactivation in normal faulting.* J.Struct. Geol., **14**, 8/9, 991-998.

Ivins E.R., Dixon T.H. & Golombek M.P., 1990 - *Extensional reactivation of an abandoned thrust: a bound on shallowing in the brittle regime.* J. Struct. Geol., **12** (3), 303-314.

Krantz R.W., 1991 - *Normal fault geometry and fault reactivation in tectonic inversion experiments.* In: *The Geometry of Normal Faults,* Geol. Soc. Spec. Publ. **56**, 219-229.

Mariotti G. & Capotorti, 1988 - *Analisi ed interpretazione di alcuni elementi tettonici recenti nella media valle del Salto (Rieti).* Rend. Soc. Geol. It., **11**, 78-94.

Mattei M., Funiciello R., Kissel C. & Laj C., 1991 - *Rotazioni di blocchi crostali neogenici nell'Appennino centrale: analisi paleomagnetiche e di anisotropia della suscettività magnetica (AMS).* Studi preliminari all'acquisizione dati del profilo CROP 11, Stud. Geol. Camerti, vol.spec. 1991, 221-230.

Mitra S. & Islam Q.T., 1994 - *Experimental (clay) models of inversion structures.* Tectonophysics, **230**, 221-222.

Montone P., 1990 - *Su alcune caratteristiche microscopiche dei piani di faglia.* Rend. Soc. Geol.It., **13**, 107-110.

Nijman W., 1971 - *Tectonics of the Velino-Sirente area, Abruzzi, Central Italy.* Koninkl. Nederl. Akad. Van Wetenshappen Proc., B **74** (2), 156-184.

Parotto M. & Praturlon A., 1975 - *Geological summary of the central Apennines.* In: *Structural model of Italy,* C.N.R. Quad. Ric. Scientifica, **90**, 257-311.

Parotto M., 1979 - *Apennin Central.* In: AA.VV.- *Géologie d'Europe.* 26° Congr. Int. di Geologia, Parigi, 198.

Parotto M; & Praturlon A., (eds)., 1975 - *Structural Model of Italy.* Quad. Ric. Scient., **90**, 257-311.

Patacca E. & Scandone P., 1990 - *Tyrrhenian basin and Apenninic arcs: kinematic relations since Late Tortonian times.* 75° Congr. Soc. Geol. It., "La geologia italiana degli anni '90" (Milano, 10-12 sett. 1990), Mem. Soc. Geol. It., **45.**

Patterson M.S., 1958 - *Experimental deformation and faulting in Wombeyan marble.* Bull. Geol.

Ranalli G. & Yin M., 1990) - *Critical stress difference and*

orientation of faults in rocks with strength anisotropies: the two dimensional case. J. Structural Geology, **12**, 1067-1071.

Royden L.H. & Burchfiel B.C., 1987) - *Thin-skinned N-S extension within the convergent Himalayan region: gravitational collapse of a Miocene topographic front.* Continental Extensional Tectonics Geological Society Special Publication, 611-619.

Salvini F., 1992 - *Tettonica a blocchi in settori crostali superficiali: modellizzazione ed esempi da dati strutturali in Appennino centrale.* In: *Studi preliminari all'acquisizione dati del profilo CROP 11,* Stud. Geol. Camerti, vol.spec. 1992, 237-248

Scheidegger A.E., 1961 - *Mathematical models of slope development.* Geol. Soc. Am. Bull., **72**, 37-50.

Sibson R.H., 1985 - *A note on fault reactivation.* J. Struc. Geol., **6**, 751-754.

Sibson R.H., 1990 - *Rupture nucleation on unfavorably oriented faults.* Bull. Seism. Soc. of Amer., **6**, 1580-1604.

Sykes L.R., 1978 - *Intraplate seismicity, reactivation of pre-existing zones of weakness, alkaline magmatism and other tectonic post-continental fragmentation.* Rev. Geophys. & Space Phys., **16**, 621-687.

White S.H., Bretan P.G. & Rutter E.H., 1986 - *Fault-zone reactivation: kinematics and mechanisms.* Phil. Trans. R. Soc. London, 317, 81-97.

Manoscritto ricevuto il 31.8.1994
Inviato all'Autore per la revisione il 11.11.1994
Testo definitivo ricevuto il 14.12.1994